Microporous Materials

DOI: 10.1002/anie.200502553

NMR Studies on the Diffusion of Hydrocarbons on the Metal-Organic Framework Material MOF-5**

Frank Stallmach, Stefan Gröger, Volker Künzel, Jörg Kärger, O. M. Yaghi, Michael Hesse, and Ulrich Müller**

The outstanding conceptual approach of so-called reticular design[1] for the generation of metal-organic frameworks (MOFs) or coordination polymers enables the tailoring of solids with regular porosity on the nanometer scale. Since the discovery of this new family of nanoporous materials, and especially stimulated by the work on MOF-5[2] as its most prominent representative, research efforts primarily focused on the synthesis and analysis of these compounds.[3,4] Research in this area is prompted by intriguing opportunities in the design of new materials by simply linking metals, which act as coordination centers, using a variety of polyatomic organic bridging ligands,[1–4] and the potential application of the resulting tailored nanoporous host materials in adsorption, separation, gas storage, and heterogeneous catalysis.[3–7] For example, the self-assembly of dicarboxylic acids of different molecular lengths as the organic linkers and octahedral basic zinc acetate clusters as the metal coordination centers leads to mechanically and thermally robust solids,[3,8,9] which may facilitate even large-scale applications of MOFs in these industrially important fields.

Industrial applications would require the removal of the organic solvent present during synthesis, which often might be difficult, as well as the introduction and diffusion of valuable (non-native) molecules in the pore space. While adsorption studies with inert gases are performed in the context of basic material characterization, similar investigations with more relevant molecules are less common. Moreover, no experimental data exist on diffusion of such molecules through the pore space of MOF materials. To our knowledge, only theoretical results on diffusion in MOF have been published so far from MD simulations of argon in MOF-2, MOF-3, MOF-5, and CuBTC,[10,11] and of other gases (H_2, N_2, CO_2) and alkanes (methane, *n*-pentane, *n*-hexane, cyclohexane, *n*-heptane) in MOF-5.[11,12] Here, we present the first experimental diffusion studies on nanoporous metal-organic framework materials. We used MOF-5 that had been prepared on a kilogram scale and studied the mobility of methane, ethane, *n*-hexane, and benzene by pulsed field gradient (PFG) NMR,[13,14] which is a well-established technique for intracrystalline self-diffusion studies in microporous solids.[14a,15–17]

The synthesis of MOF-5 by an optimized large-scale preparation, the removal of organic solvent, and sample characterization by wet chemical analysis, adsorption studies (including isotherms of argon, methane, and ethane), X-ray diffraction, and solid-state ^{1}H(MAS) NMR are described in the Supporting Information. The results show the characteristics expected for MOF-5,[1,4] and there is no evidence that the material decomposes during the experiments. Electron micrographs of the obtained MOF-5 material, which has a specific surface area of 3400 $m^2 g^{-1}$, show well-shaped, high-quality cubic crystals with crystal sizes between 50 to 200 μm (Figure 1). They are sufficiently large to measure intracrystalline self-diffusion by PFG NMR. For these diffusion studies, volumetrically determined amounts of the sorbate gases (vapors) were adsorbed at 77 K onto activated MOF-5 samples in NMR sample tubes (Table 1). The absorbed amounts correspond to about five (benzene, *n*-hexane) and six (methane, ethane) carbon atoms of the adsorbate molecule per cavity of the MOF-5.

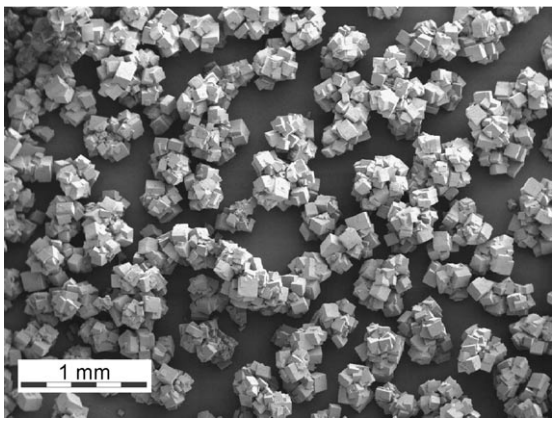

Figure 1. Scanning electron micrograph (SEM) of MOF-5 crystals obtained from the optimized large-scale preparation. The bar represents a length of 1 mm.

PFG NMR measurements were performed on the custom-built NMR spectrometer Fegris 400NT[18] using the 13-interval stimulated spin-echo pulse sequence with two pairs of alternating pulsed magnetic field gradients (amplitude g, width Δ) for diffusional encoding.[19] This technique is

[*] Dr. habil. F. Stallmach, S. Gröger, V. Künzel, Prof. J. Kärger
Fakultät für Physik und Geowissenschaften
Universität Leipzig
Linnèstrasse 5, 04103 Leipzig (Germany)
Fax: (+49) 341-973-2549
E-mail: stallmac@physik.uni-leipzig.de
Dr. M. Hesse, Dr. U. Müller
BASF Aktiengesellschaft
GCC/Z – M301, 67056 Ludwigshafen (Germany)
Fax: (+49) 621-605-6190
E-mail: ulrich.mueller@basf-ag.com
Prof. O. M. Yaghi
Department of Chemistry, University Michigan
930 North University Avenue
Ann Arbor, MI 48109-1055 (USA)

[**] This work was supported by the German Science Foundation (DFG) through the International Research Training Group "Diffusion in Porous Materials". We are grateful to two referees for their suggestions to include solid-state NMR data. We thank M. Wehring and W. Böhlmann (Leipzig) for acquiring these data.

Supporting information for this article is available on the WWW under http://www.angewandte.org or from the author.

Table 1: Effective (D_{eff}) and intracrystalline self-diffusion coefficients (D_1, D_2) of hydrocarbons in MOF-5 for selected temperatures as measured by PFG NMR spectroscopy.[a]

Adsorbate	Loading [mg g^{-1}]	T [K]	Δ [ms]	D_{eff} [m^2 s^{-1}]	D_1 [m^2 s^{-1}]	D_2 [m^2 s^{-1}]	p_1 [%]	p_3 [%]
methane	120	298	5...40	$\approx 2.0\times10^{-6}$	$\approx 1.7\times10^{-7}$			
		173	5...80	1.9×10^{-7}	1.2×10^{-8}			
ethane	120	298	5...40	2.0×10^{-7}	2.1×10^{-8}			
		223	5...80	1.4×10^{-8}	1.9×10^{-8}	4.7×10^{-9}	60	1.2
n-hexane	100	298	10...20	1.8×10^{-9}	3.2×10^{-9}	4.0×10^{-10}	50	6.5
			40...80	2.6×10^{-9}	4.1×10^{-9}	4.5×10^{-10}	59	7.0
benzene	80	298	10...40	1.3×10^{-9}	1.8×10^{-9}	3.5×10^{-10}	72	1.5
			80	1.4×10^{-9}	2.0×10^{-9}	4.0×10^{-10}	60	2.5

[a] For ethane (at 223 K), *n*-hexane, and benzene, the intracrystalline diffusivities D_1 and D_2, and the percentages of fast-diffusing (p_1) and nondiffusing (p_3) fractions of the multiexponential fits displayed in Figure 2c, e, and f are given. For *n*-hexane and benzene for different observation times Δ slightly different fit parameters result.

primarily sensitive to the mean square displacement $\langle r^2(\Delta)\rangle$ of molecules during the time Δ between the pairs of pulsed field gradients, which is referred to as observation or diffusion time. For all adsorbates, the spin-echo intensity $M(b)$ was observed as a function of the parameter b, which is defined by $b=(\gamma g 2\delta)^2(\Delta-{}^1\!/_6\delta-{}^1\!/_2\tau)$.[19] Characteristic values of the experimentally varied gradient parameters (g, δ, Δ) and the radio-frequency pulse distance τ are summarized in the Experimental Section. Self-diffusion coefficients ($D=\langle r^2(\Delta)\rangle/(6\Delta)$) and information on diffusional exchange between gas and adsorbed phase during Δ were obtained by analyzing the slope and the shape of the plot of $\ln(M(b)/M_0)$ versus b, respectively.[13–17] To determine where the observed diffusion process takes place, the dependence of the spin-echo attenuation on observation time as well as on temperature was studied.

Figure 2 shows examples of such spin-echo attenuations in MOF-5. All plots of $\ln(M(b)/M_0)$ versus b deviate from linearity, which indicates a distribution of self-diffusion coefficients. Methane at all temperatures and ethane at the higher temperature show decreasing amounts of slowly decaying signal fractions with increasing diffusion time. Such behavior is well known from diffusion studies in zeolites,[16,17] where the different mobilities of the adsorbent molecules in intra- and intercrystalline space are detected by PFG NMR spectroscopy. This feature of PFG NMR spectroscopy is utilized by the fast NMR tracer exchange method to determine the fraction of molecules remaining during the diffusion time in the intracrystalline space, their self-diffusion coefficient D, and their mean intracrystalline lifetime τ_{intra}.[16,17] The curves in Figure 2a, b, and d are compatible with this fast tracer exchange method and were analyzed accordingly: The slope of the linear regression of the slowly decaying signal fraction yields the intracrystalline self-diffusion coefficient D. Its extrapolation to $b=0$ determines the relative amount $a(\Delta)$ of molecules remaining during the diffusion time only in the intracrystalline space. The regression lines and their interpolations are included in Figure 2a, b, and d.

In Figure 3 the temperature dependence of the intracrystalline self-diffusion coefficients for methane and ethane are shown and compared with corresponding values of self-diffusion in NaX zeolites.[20] Clearly, diffusion of methane and ethane in MOF-5 is faster than in NaX. This might be a consequence of the difference between the diameters of the large nanoporous cavities in MOF-5 (1.5 nm) and in NaX (1.2 nm).

The pronounced dependence of the spin-echo attenuation on the observation time (Figure 2a, b, and d) shows that methane and ethane exchange between intracrystalline and intercrystalline space already on the millisecond time scale of the PFG NMR experiment. Figure 4 plots the relative amounts $a(\Delta)$ of molecules diffusing only in the intracrystalline space as function of the diffusion time. These values decrease with increasing diffusion time, since more and more molecules reach

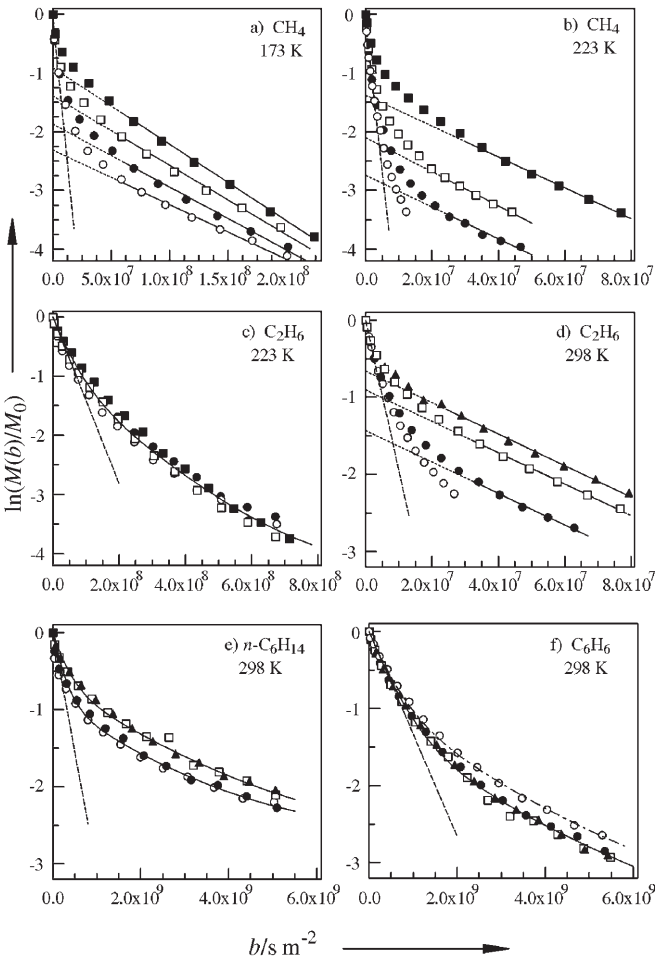

Figure 2. PFG NMR spin-echo attenuation ($\psi(b)$) and data analysis for: a,b) methane, c,d) ethane, e) *n*-hexane, and f) benzene in MOF-5 for observation times $\Delta=5$ ms (■), 10 ms (▲), 20 ms (□), 40 ms (●), and 80 ms (○), respectively. Dashed lines represent the initial decays yielding the effective self-diffusion coefficients. In the time-dependent decays of parts a, b, and d, solid and dotted lines represent linear regressions and their interpolations to $b=0$ in order to determine the intracrystalline self-diffusion coefficient D and lifetimes τ_{intra}. For attenuations observed in parts 2c, e, and f, fits using a multiexponential model are included.

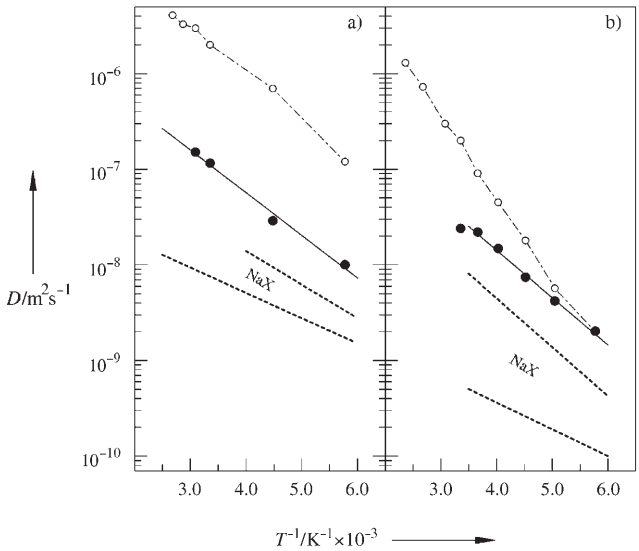

Figure 3. Arrhenius presentation of the intracrystalline (●) and effective (○) self-diffusion coefficients of: a) methane and b) ethane in MOF-5. The region between the dotted lines shows the range of intracrystalline self-diffusion coefficients in NaX zeolite for loadings from about 30–90 mg g^{-1} methane (part a) and 110 mg g^{-1} ethane (part b), respectively.[20] The solid lines correspond to activation energies of 8.5 kJ mol^{-1} (methane, part a) and 9.5 kJ mol^{-1} (ethane, part b) for adsorbate self-diffusion in MOF-5.

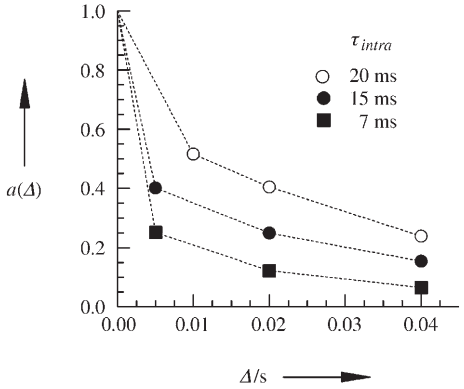

Figure 4. Relative amount $a(\Delta)$ of molecules that diffuse during the time interval Δ only in the intracrystalline space of MOF-5. Data are obtained for methane (● 173 K; ■ 223 K) and ethane (○, 289 K) from linear extrapolation of the PFG NMR spin-echo attenuations in Figure 2a, b, and d. They decrease with increasing Δ and, thus, give evidence for fast exchange between inter- and intracrystalline space. The dotted lines represent linear interpolations between the data points. Estimates for the mean intracrystalline lifetime τ_{intra} are included into the legend.

the crystal boundary and contribute to this exchange. The mean lifetime τ_{intra} of a diffusing molecule in the intracrystalline space is obtained by integrating over $a(\Delta)$.[16,17] The τ_{intra} values reported in Figure 4 were estimated by the area under the linear interpolation between the experimental data and are thus only rough estimates. Nevertheless, the results demonstrate that light hydrocarbons easily exchange between the intracrystalline phase in MOF-5 and the surrounding gas phase. Above room temperature this exchange is so fast that intracrystalline diffusion cannot be observed by PFG NMR spectroscopy. Therefore, for higher temperatures only the effective self-diffusion coefficients, which represent the long-range diffusion through the bed of MOF-5 crystals, are plotted in Figure 3.

Spin-echo attenuations for ethane at low temperatures as well as for *n*-hexane and benzene at room temperature (Figure 2c, e, and f) are qualitatively different from those discussed above. Within the experimental uncertainty, the observed decays do not depend on observation time Δ but are again nonlinear with b. This indicates a distribution of self-diffusion coefficients that is independent of observation time. Thus, regions with different adsorbate mobilities must exist within the MOF-5 sample, and the molecules do not exchange between these regions during the time scale of the NMR experiment. For quantitative analysis, the initial decay of the spin-echo attenuation was evaluated (see dashed lines in Figure 2). It yields the effective self-diffusion coefficient D_{eff}, which—regardless of the underlying distribution—coincides with the arithmetic mean diffusion coefficient. Additionally, the whole spin-echo attenuation curve is fitted by assuming a multiexponential decay yielding two diffusion coefficients ($D_i > 0$, $i = 1, 2$) with relative contributions p_i and a constant, nondiffusing ($D_3 = 0$) background contribution p_3. Solid lines in Figure 2c, e, and f represent the fits using this multi-exponential model. The effective self-diffusion coefficients and the results of the multiexponential model are given in Table 1.

The effective self-diffusion coefficients of *n*-hexane and benzene in the MOF-5 structure are only slightly smaller than their values in the neat liquids at the same temperature (C_6H_6: 2.21×10^{-9} m^{2}s^{-1}; C_6H_{14}: 4.26×10^{-9} m^{2}s^{-1}[21]). On the basis of the low loadings, visual inspection of the samples, and the absence of the typically long transverse relaxation time components of liquids, the presence of liquid droplets of *n*-hexane and benzene outside the MOF-5 crystals must be excluded. Thus, the presented effective diffusivities represent averaged intracrystalline mobilities. The multiexponential analysis shows that about 50–70% of the adsorbed molecules have liquidlike high mobilities. The residual fractions show significantly lower self-diffusion coefficients (see Table 1). The micropores in fractions of the MOF-5 crystals may be partially blocked by residual solvents or structural defects. Both effects reduce intracrystalline mobilities and may thus lead to a distribution of self-diffusion coefficients of adsorbed *n*-hexane, benzene, and even ethane (at low temperatures) as evidenced in the PFG NMR experiments.

The presence of about 0.2 molecules of the solvent diethylformamide (DEF) per cavity of the MOF-5 even after activation at 100 °C was observed by solid-state ^{1}H MAS NMR spectroscopy (see the Supporting Information). These residual DEF molecules are most likely the reason for the two signal fractions with reduced mobility, observed by PFG NMR spectroscopy owing to 1) their influence on a part of the adsorbed molecules and 2) their own contribution to the ^{1}H NMR signal observed.

With regard to point (1): The DEF molecules occupy pore space and may even block windows between MOF-5 cavities.

This reduces adsorbate mobility and leads to the second component (D_2 in Table 1), in addition to the first component (D_1 in Table 1) represented by the adsorbate molecules in MOF-5 regions which are locally free of residual solvent molecules. The absence of diffusional exchange between the regions of different DEF content as evidenced in the *n*-hexane, benzene, and low-temperature ethane data suggests that these regions are macroscopically separated; that is, DEF molecules are not distributed homogeneously throughout the MOF-5 material. For example, since the applied washing procedures are more effective for the outer crystal regions, it could be that central regions of the large crystals contain a higher DEF concentration than the outer regions.

With regard to point (2): The ethyl groups of the residual DEF molecules contribute to the PFG NMR spin-echo signal, which is evidenced by the static ^{1}H NMR spectra of the activated samples presented in the Supporting Information. Since these DEF molecules are obviously strongly attached to the MOF-5 lattice, their signal is not attenuated in the PFG NMR experiment yielding the third, nondiffusing signal fraction (component p_3 in Table 1).

Regardless of their origins, both signal fractions with reduced mobilities do not influence significantly the overall fast effective diffusivities measured for the adsorbates in MOF-5. In the future, detailed investigations by solid-state NMR spectroscopy in combination with PFG NMR spectroscopy are desirable to quantify the effect of the solvent molecules on diffusion studies of guest molecules in nanoporous metal-organic framework materials.

For *n*-hexane, the fast component of intracrystalline diffusivity ($3.2–4.1\times10^{-9}\,m^2\,s^{-1}$, see Table 1) is in good agreement with the value of $2.2\times10^{-9}\,m^2\,s^{-1}$[12] predicted by MD simulation for a slightly higher loading. For methane, the intracrystalline self-diffusion coefficient measured by PFG NMR spectroscopy is about one order of magnitude higher than the value of $3.1\times10^{-8}\,m^2\,s^{-1}$[11,12] reported in MD simulations. This discrepancy might have its origin in the much lower loadings used in the MD simulations and/or in imperfections in the micropore structure which influence the experimental PFG NMR studies but which are not taken into account in the MD simulations. To our knowledge, there are no other diffusion data from metal-organic frameworks available for direct comparison between the two methods.

In conclusion, we have demonstrated for the first time the superior diffusional properties of organic gas molecules in the metal-organic framework compound MOF-5. The unique combination of high porosity with record number surface area and regular nanometer pores and the absence of nonpenetrable bulk matter might lead to interesting features for industrial gas processing and storage. The high gas molecule mobility in MOF-5 and its fast exchange with the surrounding gas atmosphere, in comparison to metal oxides, zeolites, carbons, resins, and numerous other materials, should result in much faster processing and lower energy consumption. In addition, the high surface area of MOF-5 of more than $3000\,m^2\,g^{-1}$ could lead to improved mass- and volume-specific gas-storage capacities thus giving lower investment costs for both stationary and mobile applications.

Experimental Section

Typical parameters for the ^{1}H PFG NMR diffusion studies with the 13-interval sequence at the Spectrometer Fegris 400NT[18] (400 MHz) were: 90°–180° radio-frequency distance $\tau = 500\,\mu s$, pulsed field gradient width $\delta = 150\,\mu s$, variable diffusion times $5\,ms \le \Delta \le 80\,ms$. Spin-echo attenuations were measured by increasing the pulsed field gradient intensity g from 0 up to a maximum value of $10\,T\,m^{-1}$. Sample temperature was controlled by a stream of air (above room temperature) or nitrogen (below room temperature) with an accuracy of $\pm$ 1 K.

Received: July 21, 2005
Revised: December 5, 2005
Published online: February 24, 2006

Keywords: alkanes · benzene · diffusion · microporous materials · NMR spectroscopy

[1] M. Eddaoudi, J. Kim, N. Rosi, D. Vodak, J. Wachter, M. O'Keeffe, O. M. Yaghi, *Science* **2002**, *295*, 469–472.
[2] H. Li, M. Eddaoudi, M. O'Keeffe, O. M. Yaghi, *Nature* **1999**, *402*, 276–289.
[3] J. L. C. Rowsell, O. M. Yaghi, *Microporous Mesoporous Mater.* **2004**, *73*, 3–14.
[4] S. Kaskel in *Handbook of Porous Solids* (Eds.: F. Schüth, K. S. W. Sing, J. Weitkamp), Wiley-VCH, Weinheim, **2002**, pp. 1190–1249.
[5] R. Q. Snurr, J. T. Hupp, S. T. Nguyen, *AIChE J.* **2004**, *50*, 1091–1095.
[6] X. Zhao, B. Xiao, A. J. Fletcher, K. M. Thomas, D. Bradshaw, M. J. Rosseinsky, *Science* **2004**, *306*, 1012–1015.
[7] O. R. Evans, H. L. Ngo, W. Lin, *J. Am. Chem. Soc.* **2001**, *123*, 10395–10396.
[8] U. Mueller, K. Harth, M. Hoelzle, M. Hesse, L. Lobree, W. Harder, O. M. Yaghi, (BASF AG), WO 03/064030, **2003**.
[9] O. M. Yaghi, M. Eddaoudi, H. Li, J. Kim, N. Rosi, (Univ. Michigan), WO 02/088148, **2002**.
[10] A. I. Skoulidas, *J. Am. Chem. Soc.* **2004**, *126*, 1356–1357.
[11] A. I. Skoulidas, D. S. Sholl, *J. Phys. Chem. B* **2005**, *109*, 15760–15768.
[12] L. Sarkisov, T. Düren, R. Q. Snurr, *Mol. Phys.* **2004**, *102*, 211–221.
[13] E. O. Stejskal, J. E. Tanner, *J. Chem. Phys.* **1965**, *42*, 288–299.
[14] a) J. Kärger, H. Pfeifer, W. Heink, *Adv. Magn. Reson.* **1988**, *12*, 1–88; b) Y. Cohen, L. Avram, L. Frish, *Angew. Chem.* **2005**, *117*, 524–560; *Angew. Chem. Int. Ed.* **2005**, *44*, 520–554.
[15] a) F. Stallmach, J. Kärger, *Adsorption* **1999**, *5*, 117–133; b) F. Stallmach, Habilitation thesis, Universität Leipzig (GE), **2004** [http://lips.informatik.uni-leipzig.de:80/pub/2004–19].
[16] J. Kärger, D. M. Ruthven, *Diffusion in Zeolites and Other Microporous Solids*, Wiley, New York, **1992**.
[17] O. Geier, R. Q. Snurr, F. Stallmach, J. Kärger, *J. Chem. Phys.* **2004**, *120*, 367–373.
[18] P. Galvosas, F. Stallmach, G. Seiffert J. Kärger, U. Kaess, G. Majer, *J. Magn. Reson.* **2001**, *151*, 260–268.
[19] R. M. Cotts, M. J. R. Hoch, T. Sun, J. T. Markert, *J. Magn. Reson.* **1989**, *83*, 252–266.
[20] J. Kärger, H. Pfeifer, M. Rauscher, A. Walter, *J. Chem. Soc. Faraday Trans. 1* **1980**, *76*, 717–737.
[21] M. Holz, H. Weingärtner, *J. Magn. Reson.* **1991**, *92*, 115–125.

